NUKLEONIKA 2007;52(1):17–27

ORIGINAL PAPER

A new method of pure ^{111}In production by proton-induced nuclear reactions with enriched ^{112}Sn

Emil Běták,
Edward Rurarz,
Stefan Mikołajewski,
Jolanta Wojtkowska

Abstract. We aimed at finding out a simple and reliable way of ^{111}In production with the highest radionuclide purity from its grand parent ^{111}Sb and parent ^{111}Sn nuclei, produced by the ^{112}Sn(p,2n)^{111}Sb and ^{112}Sn(p,pn)^{111}Sn reactions, respectively. The target was a metallic ^{112}Sn sample enriched to 84%. We have measured activation cross sections for seven reactions on an enriched ^{112}Sn sample induced by 23.6 ± 0.8 MeV energy protons. Gamma-ray spectroscopy with high-purity germanium detectors has been used. We also identified the activities of ^{55}Co ($T_{1/2}$ = 17.5 h) and ^{60}Cu ($T_{1/2}$ = 23.7 min) in proton beam monitoring Ni foils, induced in the ^{nat}Ni(p,X)^{55}Co and ^{nat}Ni(p,X)^{60}Cu reactions at 22.8 MeV proton energy. The cross sections determined for these reactions are: σ[^{nat}Ni(p,X)^{55}Co] = 36.6 ± 4 mb and σ[^{nat}Ni(p,X)^{60}Cu] = 64.4 ± 7 mb. The measured cross sections of reactions on tin isotopes are: σ[^{112}Sn(p,n)^{112}Sb] = 4 ± 0.8 mb; σ[^{112}Sn(p,2n)^{111}Sb] = 182 ± 26 mb; σ[^{112}Sn(p,pn)^{111}Sn] = 307 ± 35 mb; σ[^{114}Sn(p,2n)^{113}Sb] = 442 ± 52 mb; σ[^{117}Sn(p,n)^{117}Sb] = 15 ± 3 mb; σ[^{117}Sn(p,p'γ)^{117m}Sn] = 0.37 ± 0.06 mb; σ[^{115}Sn(p,2p)^{114m2}In] = 0.01 ± 0.002 mb. Our measurements indicated the expected yield of the ^{111}In production to be 46 MBq/μAh (1.2 mCi/μAh). The contamination of ^{111}In by the undesired nuclide ^{114m2}In was determined and belongs to the smallest ones found in the literature. The measured cross sections were compared with theoretical calculations by two top-level nuclear reaction codes EMPIRE and TALYS.

Key words: cross sections • Sn isotopes • proton-induced reactions • ^{111}In production • diagnostic radioisotope

E. Běták✉
Institute of Physics, Slovak Academy of Sciences,
84511 Bratislava, Slovakia
and Faculty of Philosophy and Sciences,
Silesian University,
74601 Opava, Czech Republic,
Tel.: +421 2 59410537, Fax: +421 2 54776085,
E-mail: betak@savba.sk

E. Rurarz, S. Mikołajewski, J. Wojtkowska
The Andrzej Sołtan Institute for Nuclear Studies,
05-400 Otwock-Świerk, Poland

Received: 14 April 2006
Accepted: 13 December 2006

Introduction

Radionuclide ^{111}In

The radionuclide ^{111}In ($T_{1/2}$ = 2.80 d, E_γ = 171.3 keV, I_γ = 90.3% and 245.4 keV, I_γ = 94%, EC 100%)[1] is widely employed in nuclear medicine for tumor imaging, labelling of lymphocytes, platelets, monoclonal antibodies and many others. Medical physicists constantly focused their attention on searching for low-cost, simple, reliable, remote- and computer-controlled production methods of ^{111}In. As ^{114m2}In ($T_{1/2}$ = 49.51 d, E_γ = 190.3 keV, I_γ = 15.0%, IT 96.75%, EC 3.25%) gives approximately 80 times the dose per the same activity of ^{111}In, it is very important to minimize the amount of ^{114m2}In impurity. The requirement for the low ^{114m2}In impurity may be formulated as "no more than 0.2% of the total radioactivity is due to ^{114m2}In at the date and hour of administration in ^{111}In" [7]. This condition is successfully satisfied in the large scale production of ^{111}In in nuclear reactions of protons with extremely enriched cadmium isotopes ^{111,112,113}Cd(p,xn)^{111}In (x = 1,2,3) at small- and medium-sized cyclotrons [32]. However, the presence of even small amounts of long-lived radioactive contaminants of ^{114m2}In in ^{111}In is of

[1] The half-lives and the isotope abundances are cited according to Ref. [30].

some concern because their emitted radiations contribute to the radiation dose to patients and they can therefore also degrade the quality of scintigraphic images. All direct nuclear reactions for the cyclotron production of ^{111}In via proton bombardment of Cd isotopes yield prohibitive amounts of ^{114m2}In. The ^{114m2}In contamination, which increases patient's radiation dose, can be effectively reduced to the level accepted by nuclear medicine, if extremely enriched targets (very close to 100%) of ^{111,112,113}In are used. Such targets are significantly more expensive than the routinely produced ones with 90–95% enrichment. In addition, the radiochemical procedures to separate ^{111}In from the target (Cd) have further disadvantages (see Ref. [32] for detailed information), so that it is highly desirable to find other methods of ^{111}In production for medical purposes.

Due to the lack of relevant nuclear data, little can be said about indirect (precursor) methods of the ^{111}In production. They use the chain decay of ^{111}Sb to ^{111}Sn parent radioisotopes formed in nuclear reactions induced by 14 MeV neutrons [4] or protons [26] with enriched ^{112}Sn sample. The irradiated ^{112}Sn sample may be considered as an ^{111}Sn $\rightarrow$ ^{111}In or ^{111}Sb $\rightarrow$ ^{111}Sn $\rightarrow$ ^{111}In precursor, from which, after appropriate waiting time, the ^{111}In isotope can be separated. Authors of Ref. [21] found a promising method for high temperature separation of ^{111}In from both small and massive (up to 50 g) tin targets exposed to protons.

In the present work, we propose a new method of no-carrier added (NCA) production of ^{111}In from its grandparent ^{111}Sb. The latter is formed at proton bombardment of an enriched ^{112}Sn target via the ^{112}Sn(p,2n)^{111}Sb $\xrightarrow[1.25\ \mathrm{min}]{\mathrm{EC},\beta+}$ ^{111}Sn $\xrightarrow[35\ \mathrm{min}]{\mathrm{EC},\beta+}$ ^{111}In reaction. Besides, the reaction ^{112}Sn(p,pn)^{111}Sn leads to the parent nuclide ^{111}Sn which decays to ^{111}In. Direct formation of ^{111}In is also possible in the ^{112}Sn(p,2p)^{111}In reaction. These three reaction channels leading to the formation of the above mentioned nuclei are shown in Fig. 1.

Furthermore, the contaminant ^{114m2}In is not produced in the ^{111}In formation during the decay of nuclei belonging to the A = 114 isobaric chain. The suggested

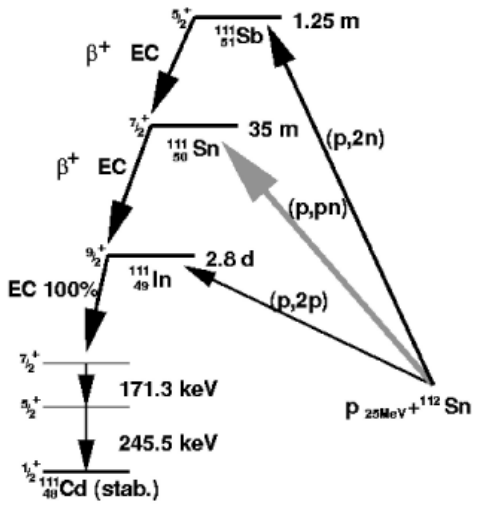

Fig. 1. Simplified decay scheme for the A = 111 nuclid series and the reaction channel leading to the formation of ^{111}Sb, ^{111}Sn and ^{111}In during the proton bombardment of the ^{112}Sn sample (based on data from Ref. [9]).

method has not received any attention of experimentalists so far.

The aim of this work was to obtain information on the ^{111}In activities induced by 25 MeV protons bombarding the ^{112}Sn target and to determine the experimental cross sections leading to the formation of desirable and undesirable radioisotopes, especially with respect to the yield and purity of ^{111}In. To our best knowledge, no data are available for these reactions below 30 MeV (with the exception of ^{117}Sn(p,n), where some data below 10 MeV have been published [8]).

The information on excitation functions of $^{112-117}$Sn isotopes is scanty and, therefore, we have implemented the codes EMPIRE and TALYS to calculate the unknown excitation functions of reactions producing unwanted radioisotopes when 25 MeV energy proton impinges on the enriched ^{112}Sn sample containing several isotopes in its vicinity.

Cross sections

The three predominant reactions in the proton energy range of interest are (p,n), (p,2n) and (p,pn), although other reactions (with the cross section of the emission of deuterons (d), tritons (t), helium-3 (τ) and helium-4 (α) by one order of magnitude lower than that of nucleon reactions named above) are also possible. The radioactive nuclides produced in the (p,n) reaction from 84% enriched ^{112}Sn and isotopic "contaminants" ^{114,115,116,117}Sn appearing in tin are ^{112,114,115,116,117}Sb. All of them have short half-lives (in comparison with 2.8 d half-life of ^{111}In), low reaction Q-values (low reaction threshold) and maxima of excitation functions around 12 to 14 MeV. For bombarding proton energy equal to 25 MeV, the cross sections are low (the "tail" of the excitation function) and consequently the induced activities are weak. Reaction (p,2n) leads to the formation of the ^{111}Sb activity, which is interesting to us, as well as to ^{113,114,115,116}Sb nuclides. The Q-values for these reactions are in the range from 13 to 18 MeV, maxima of excitation functions are in the energy range 20 to 25 MeV and cross sections in these maxima are few hundred millibarns. All (p,n) and (p,2n) reaction products on tin isotopes in our sample have short half-lives and do not represent any risk for radioisotope purity of ^{111}In. Very interesting reaction for the ^{111}In production purposes is the (p,pn), producing the ^{111}Sn (parent of ^{111}In) from the ^{112}Sn isotope (main component of the sample). Besides ^{111}Sn (which decays to ^{111}In), also the long-lived ^{113}Sn ($T_{1/2}$ = 115 d) is formed in the ^{114}Sn(p,2n) ^{113}Sb $\rightarrow$ ^{113}Sn $\rightarrow$ ^{113m}In and the ^{114}Sn(p,pn) ^{113}Sn $\rightarrow$ ^{113m}In reactions. The presence of the ^{113}Sn/^{113m}In pair (well known in nuclear medicine) does not affect the quality of produced ^{111}In, since the ^{113}Sn radioisotope remains in the target material after chemical separation. The ^{114,115,116}Sn isotopes produced by the (p,pn) reaction from ^{115,116,117}Sn isotopes are stable. Similar considerations apply to the indium isotopes formed in the (p,2p) reaction. Of the total of five isotopes of indium that are formed, two of them, namely ^{113,115}In, are stable, the ^{111}In radioisotope is formed directly, but its production is rather low (as a result of small cross section and

consequently with low activity). Further on, $^{116m,\gamma}$In is short-lived both in its ground state and as an isomer. Finally, the unwanted (contaminant) ^{114m2}In isomeric activity is not significantly produced due to the long half-life (50 days) as well as due to rather low cross section of the (p,2p) reaction in this mass region. Because the natural isotopes of tin have adjacent mass numbers, the same radioactive products are sometimes produced by different reactions. For example, ^{114}Sb may be produced via ^{114}Sn(p,n)^{114}Sb and ^{115}Sn(p,2n)^{114}Sb. The possibility to induce the ^{112,114,115,116,117}Sn(p,xn yp $z\alpha$)^{111}In reactions has not yet been considered to our knowledge. The role of nuclear reaction cross-section data in optimisation of production methods, especially with respect to the yield and purity of the desired product is well established.

Methods

Targetry and cyclotron irradiations

All irradiations of the samples were performed using the C-30 cyclotron of the A. Sołtan Institute for Nuclear Studies, Świerk. Negative H-ions were accelerated and, when both electrons were stripped off on an Al foil, they were directed to the beam line. The latter consists of two steering magnets (M), two quadrupole lenses (Q_1 and Q_2), system of slits and a small diagnostic chamber equipped with a $\Delta E + E$ semiconductor Si(Li) telescope, which is followed by a thick Si(Li) detector (also working as spectrometer) for measuring (monitoring) proton beam intensities (see Fig. 2).

The energy of the proton beam was measured with a polyethylene foil working as a proton scatterer. The peak due to elastic scattering by ^{12}C (constituent of the polyethylene foil) and few peaks corresponding to inelastically scattered protons were measured with the calibrated $\Delta E + E$ semiconductor Si(Li) telescope. It was found that the proton energy after passing a cyclotron vacuum isolation foil was 25.0 ± 0.2 MeV. Samples of enriched ^{112}Sn and natural tin were metallic plates shaped in the form of discs. Isotopic composition in the used enriched ^{112}Sn target in % was: ^{112}Sn (84), ^{114}Sn (13), ^{115}Sn (0.75), ^{116}Sn (2) and ^{117}Sn (0.25). Both targets, the 84% enriched ^{112}Sn with mass 20.6 mg and natural tin with mass 31.5 mg were cut into discs with 5 mm in diameter and thicknesses 0.2 mm and 0.26 mm, respectively. Practically all charged particle beam power (energy × current) deposited in the target is dissipated as heat. Tin has low melting point, so we performed a series of irradiations with natural tin in order to establish safe irradiation conditions for our enriched sample. The proton beam current was measured with a Faraday cup and a calibrated current integrator. Additionally, the integrated proton beam intensities were monitored by passing the beam through a high purity Cu metal foil, 0.03 mm thick (in front) and a 0.02 mm thick Ni foil (in the back) of the ^{112}Sn target. Copper and nickel were chosen as monitoring material since many reaction products can be determined easily by gamma-ray spectroscopy, as excitation functions for these reactions are well known [1, 11, 12, 16, 19, 20, 27–29]. The diameter of the beam striking the first (Cu) foil and the next ^{112}Sn and Ni foils was defined by the collimator aperture to 5 mm (Fig. 3).

All three samples (^{nat}Cu, ^{112}Sn, ^{nat}Ni) were placed one behind the other in a stack-like arrangement along the axis of the uniformly diffused proton beam.

Thin foils of some metals of low melting point, like Zn, Sn, In and some others, are forbidden to be irradiated inside the vacuum chamber of the cyclotron, as their vapours may cause breakdown of the cyclotron chamber. Therefore, the incident 25 MeV proton energy passing through a small air path bombarded the Cu foil leading to the production of ^{62,63}Zn and ^{61,64}Cu activities. That also enabled us to use simple, cheap and reliable hand transport of irradiated samples. The energy loss in the 0.03 mm thick copper foil amounted to 0.58 MeV at a proton energy of 25 MeV (energy loss according to Williamson *et al.* [31]). The outgoing protons from the Cu foil with energy 24.42 MeV bombarded then a ^{112}Sn sample and excited ^{111,112,113,114,115,116,117}Sb, ^{111,113}Sn and ^{111,114,116}In activities. After passing the 0.2 mm thick ^{112}Sn sample, the proton energy was degraded by further 1.59 MeV. Due to great proton energy degradation in tin sample, the mean energy of an irradiation was taken as the proton energy at the center of the target foil and equal to 23.6 ± 0.8 MeV. Protons going out from the ^{112}Sn sample with energy 22.83 MeV bombarded the second monitoring foil made of nickel and excited ^{55,57}Co, ^{57}Ni, ^{60,61}Cu activities. They additionally lost 0.35 MeV at proton penetration through the 0.02 mm thick nickel foil and were afterwards stopped in the Faraday cup located behind the irradiated samples. The determination of the average beam flux on the targets

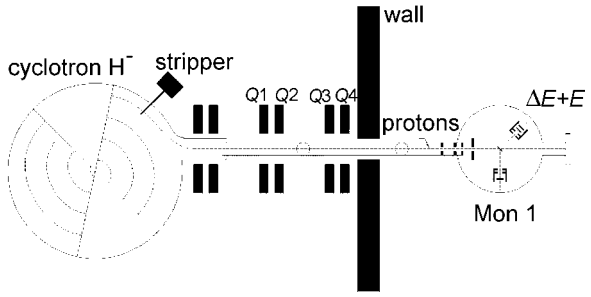

Fig. 2. Sketch of cyclotron and proton beam line. The dipoles M and the quadrupole Q focusing lenses are marked as well as the positions of the proton monitors and telescope detector are shown.

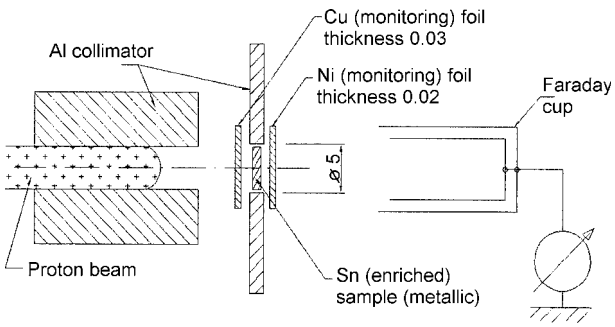

Fig. 3. Scheme of the irradiation arrangement. The 25 MeV proton beam passes through the Cu monitoring foil and then through the enriched metallic ^{112}Sn sample and finally through the Ni monitoring foil.

was performed by integrating the current measured in the Faraday cup and checked by the results obtained from ^{nat}Cu and ^{nat}Ni monitor reactions. The mean effective beam energies in the ^{nat}Cu,^{112}Sn, ^{nat}Ni foils along the stack were calculated using the range and stopping power tables [15] and by fitting to the well known excitation functions of monitoring elements.

In order to induce mainly the ^{111}Sb activity ($T_{1/2}$ = 75 s), the duration of bombardment of tin samples was kept at 5 min (4 × 75 s = 5 min), as this is optimal time for ^{111}Sb activity to reach saturation. In the case of induction of the ^{111}Sn activity ($T_{1/2}$ = 35 min), the duration of proton bombardment was kept at 1 h (about 2 × $T_{1/2}$ of ^{111}Sn). The proton beam intensity was limited to 27 nA during 5 min and 3.5 nA during 1 h irradiations due to the lack of cooling of tin samples. The beam current was stable at each irradiation.

Gamma-ray measurements

Following the irradiation of targets, the gamma rays were detected by two high purity germanium (HPGe) detectors. Gamma spectra of residual activities in the ^{112}Sn target and in monitor foils (Cu, Ni) have been collected with a HPGe detector (Canberra, Model GMX3520, carbon epoxy window, 2.0 keV energy resolution at 1332 keV and 1.1 keV at 122 keV, respectively) connected via a linear amplifier (Tennelec TC245) to a 4096 channel computerized multichannel analyzer. Twenty two successive 4096 channel spectra were measured with this spectrometer. The duration of measuring time and intervals varied with the activity investigated. Majority of measurements were performed with this spectrometer (with known detector efficiency) when the distance between the irradiated sample and detector was 3 mm. From our preliminary measurements, one could expect the ^{111}Sn activities about 2.5 MBq (70 μCi). Because of this higher activity, it was necessary to increase the sample-to-detector distance to 29 cm in order to decrease the deadtime and γ-γ and *x*-γ sum effects and to determine the absolute detector efficiency.

The ^{114m2}In in our irradiated samples was measured by us and independently at the Metrological Laboratory of Radioactive Materials (MLRM) of the Radioisotope Centre Polatom at Świerk with an HPGe detector (Canberra GC1520, 72 cm^3 volume, 1.8 keV energy resolution for 1332 keV line) connected to a computerized spectrometric system. The data on both spectrometric systems were processed using the GENIE-2000 program [10]. The induced activities in the ^{112}Sn sample were followed over a period of two months. Such long interval allowed us to determine the ^{114m2}In contamination level. Observed activities were then used to determine the cross sections and the production yields. The cross sections were calculated using standard activation formula. Preliminary information about the activities encountered in the activation of the 84% enriched ^{112}Sn sample by 25 MeV protons can be obtained from analysis of Ref. [26] and Table 1.

Table 1. *Q*-values and decay properties of nuclides produced by 25 MeV protons induced reactions on ^{112}Sn and on its $^{114–117}$Sn impurities (*Q*-values (MeV) from Ref. [2], half-lives from Ref. [30])

Target isotope and its abundance in the enriched target	Reaction				Comment
	(p,n)	(p,2n)	(p,pn)	(p,2p)	
^{112}Sn (84%)	^{112}Sb	^{111}Sb	^{111}Sn	^{111}In	product nucleus
	–7.842	–16.659	–10.787	–7.554	*Q*-value
	51.4 s	75 s	35.3 min	2.805 d	half-life
	β$^+$, EC	β$^+$, EC	EC	EC	decay mode
^{114}Sn (13%)	^{114}Sb	^{113}Sb	^{113}Sn	^{113}In	product nucleus
	–6.828	–15.027	–10.299	–	*Q*-value
	3.49 min	6.67 min	115.1 d	–	half-life
	β$^+$, EC	β$^+$, EC	EC	stable	decay mode
^{115}Sn (0.75%)	^{115}Sb	^{114}Sb	^{114}Sn	^{114}In	product nucleus
	–3.815	–14.407	–	–8.753	*Q*-value
	32.1 min	3.49 min	–	49.51 d (IT), 71.9 s (G)	half-life
	β$^+$, EC	β$^+$, EC	stable	β$^+$, β$^-$, EC	decay mode
^{116}Sn (2%)	^{116}Sb	^{115}Sb	^{115}Sn	^{115}In	product nucleus
	–5.489	–13.411	–	–	*Q*-value
	60.3 min (IT) 15.8 min (G)	32.1 min	–	–	half-life
	β$^+$, EC	β$^+$, EC	stable	stable	decay mode
^{117}Sn (0.25%)	^{117}Sb	^{116}Sb	^{116}Sn	^{116}In	product nucleus
	–2.537	–12.465	–	–9.439	*Q*-value
	2.80 h	60.3 min (IT) 15.8 min (G)	–	2.18 s (IT), 54.3 min (IT) 14.1 s (G)	half-life
	β$^+$, EC	β$^+$, EC	stable	β$^-$	decay mode

Gamma transitions and cross sections

Two γ-lines from ^{112}Sb decaying with energies 990.9 and 1257.1 keV were used to determine the ^{112}Sn(p,n)^{112}Sb cross section. The 154.1 keV γ-ray emitted in the decay of short-lived ^{111}Sb was used to deduce the ^{112}Sn(p,2n)^{111}Sb cross section. The cross section of the ^{112}Sn(p,2n)^{111}Sb reaction was obtained from the 154.1 keV γ decay of short-lived ^{111}Sb. This reaction is very important for the estimation of the induced ^{111}Sb (grand parent) activity in radioisotope precursor and, therefore, a precise excitation function for this reaction is required. Another short-lived activity, namely that of ^{113}Sb, was identified via its 498 keV line. The ^{111}Sn ($T_{1/2}$ = 35 min) nucleus (parent of ^{111}In) has a large number of γ transitions, including some high energy ones, which makes it easy to detect and identify. Not many γ-lines of the ^{111}Sn decay are of higher intensities, however. The cross section of the ^{112}Sn(p,pn) ^{111}Sn reaction was measured using two of them, namely the 762 and 1153 keV. The half-life of ^{111}Sn (for identification purpose) was determined from the decay of these two lines, which are a part of eight successive spectra.

The ^{111,112,113,117}Sb, ^{111,117m}Sn and ^{114m}In activities in the enriched ^{112}Sn sample were easily identified via observation of their known gamma lines with identifiable half-lives.

The absolute detector efficiency calibration in the energy region below 2 MeV was performed using standard mono- and multi-line calibrated sources manufactured at MLRM. The intensities per decay of used γ-rays were taken from Refs. [9, 22–24].

The absolute detector efficiency for different γ-ray energies is shown in Fig. 4. We have performed an interlaboratory comparison of activities determined using both detectors, and it showed very good agreement of the results of independently measured samples. This excluded the error in detector calibration.

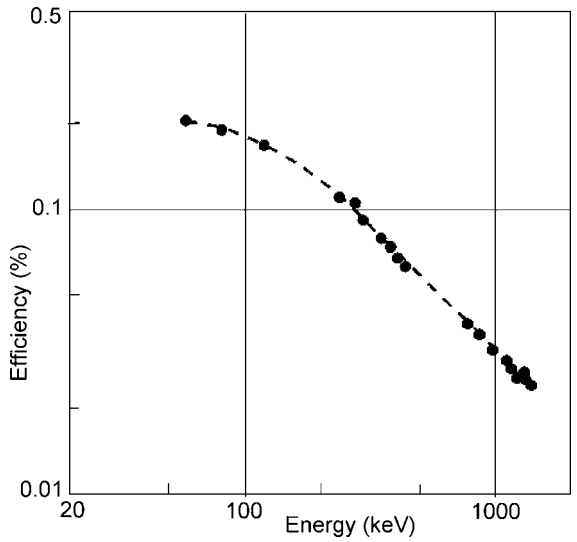

Fig. 4. Absolute photopeak efficiency of the HPGe detector (Canberra, GMX3520, carbon epoxy window) measured at a detector-source distance of 29 cm using calibrated ^{60}Co, ^{133}Ba, ^{152}Eu and ^{241}Am sources.

Cross section calculations

In order to have some information on the incident energy dependence of the cross sections, we have calculated the excitation functions. At energies of our cyclotron, it is necessary to take into account also the pre-equilibrium effects in addition to the traditional approach of compound nucleus concept and/or direct reactions. Recently, two codes that include the whole range of approaches and are also coupled to extensive libraries of parameters, have been released, namely EMPIRE-II (version 2.18 Mondovi in 2002 [13] and the version 2.19 Lodi [14] one year ago)[2] and the TALYS code written by another group [18].

These codes are very close as for their underlying physics at the pre-equilibrium stage (e.g., the same single-nucleon radiative mechanism formula for the γ emission is used both in EMPIRE and in TALYS), and similarly both of them use very extensive tables of various recommended parameters.

The main differences important for the pre-equilibrium stage of the reaction may be summarized (see also [3]): i) the basic approach to the pre-equilibrium stage is the two-component one (i.e. distinguishing between the neutrons and the protons) in TALYS, whereas one-component formulation with a charge factor is used in EMPIRE; ii) one-particle radiation mechanism for the γ emission is used in EMPIRE, but TALYS adds the quasideuteron (two-particle) one[3], what may cause some differences (however, very small ones) at excitation energies above about 30 MeV; iii) though the level densities (using the default option) are the same in both codes (with parameters taken from RIPL [25]), different (semi-)microscopic approaches are available for the advanced user; iv) classical optical model with deformed potential is used to calculate the particle transmission coefficients T_l in EMPIRE with parameters from libraries, and the local and global parameterization of [17] is employed in TALYS. (This difference influences the γ emission only via the competition with that of the particles.) Both codes have been used with near-default parameters, just with stressing the possibility of the pre-equilibrium emission which is significant at our energies (for the details, see [3]), to generate the unknown excitation functions of these reactions [26]. The calculated excitation functions do not claim to be exact, as we are rather far off the valley of β stability, and the specific properties of included nuclei necessary for the calculations are not known with sufficient precision. Anyway, they give reasonable estimates of the shapes of excitation functions, the positions of their maxima and also on the cross sections.

[2] The main differences between these two versions of EMPIRE-II can be summarized as replacing the data libraries by their more recent versions, adding of further subprograms and subroutines and also correcting of some minor bugs.

[3] The quasideuteron mechanism is also included in EMPIRE-II v. 2.19, but it is considered for the photonuclear reactions only, and not for the γ emission.

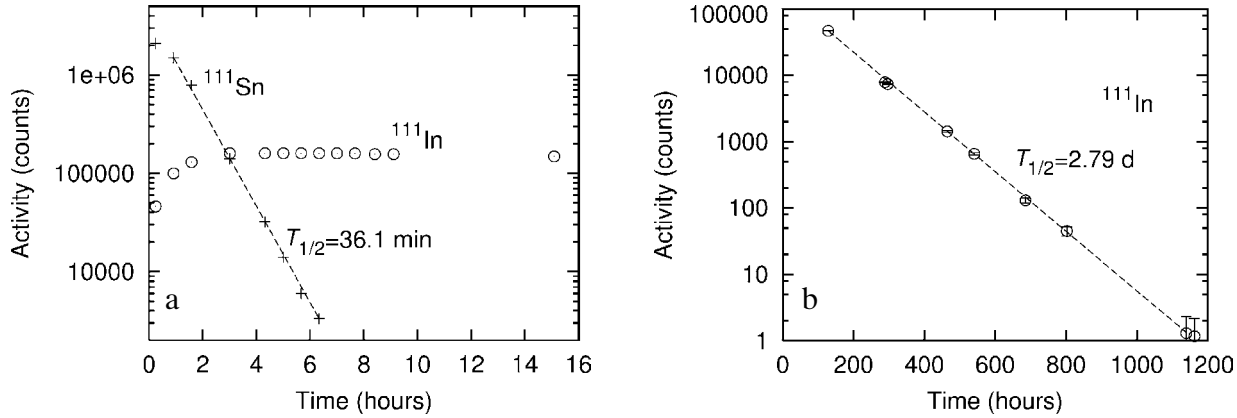

Fig. 5. Half-life analysis of the strongest photopeaks (762 and 1153 keV) in the decay of ^{111}Sn. We can see also an increase of ^{111}In activity (a) and its decay (b). The measurement of the ^{111}In activity (up to the last point on the right part) are our results, whereas the decay of ^{111}Sn and the last point of ^{111}In (at 1162.6 hrs) are the data of the Metrological Laboratory of the Radioactive Materials Radioisotope Centre, Polatom, Świerk.

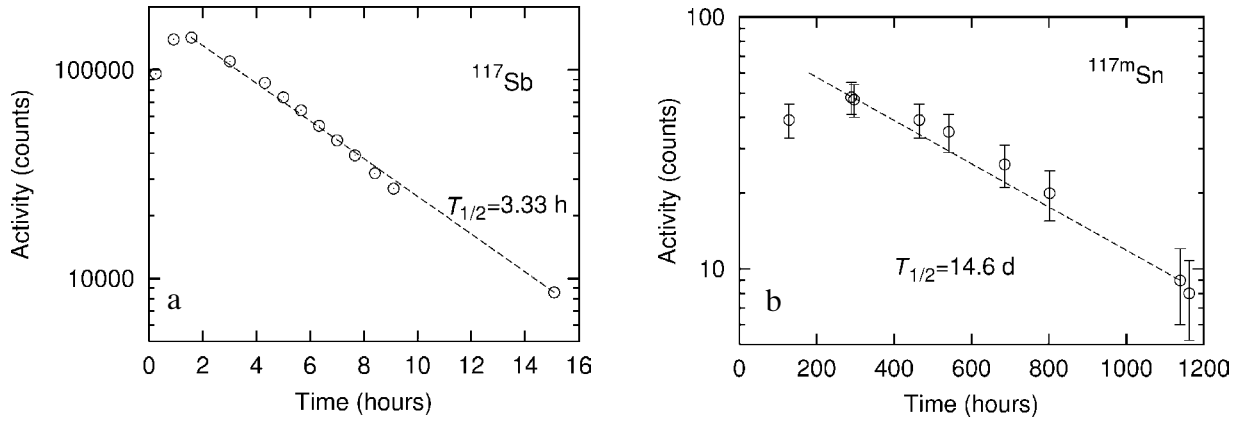

Fig. 6. Decay of the 158 keV gamma-ray activity produced in the ^{117}Sn(p,n)^{117}Sb reaction (a) and in the ^{117}Sn(p,p'γ)^{117m}Sb inelastic scattering (b) of 23.6 MeV protons on ^{117}Sn, constituent of 84% enriched ^{112}Sn sample.

Results

Experimental results

The analysis shown in Fig. 5 yields the value $T_{1/2}$ = 36.1 ± 0.4 min for ^{111}Sn, which agrees with Refs. [9, 22–24, 30] data. In addition to the ^{111}Sn decay, Fig. 5 shows also the growth and decay of the ^{111}In activity (measured using 171.3 and 245.4 keV γ-lines).

Figure 6 shows the decay of the 158 keV peak γ activity. The long-lived component is due to ^{117m}Sn and the short-lived one to ^{117}Sb. A straight line is drawn through the experimental points to fit the previously measured half-lived of ^{117}Sb and ^{117m}Sn [24].

Our experimental cross sections measured at 23.6 MeV are shown in Figs. 7 and 8, together with the calculated excitation functions for incident energies below 30 MeV.

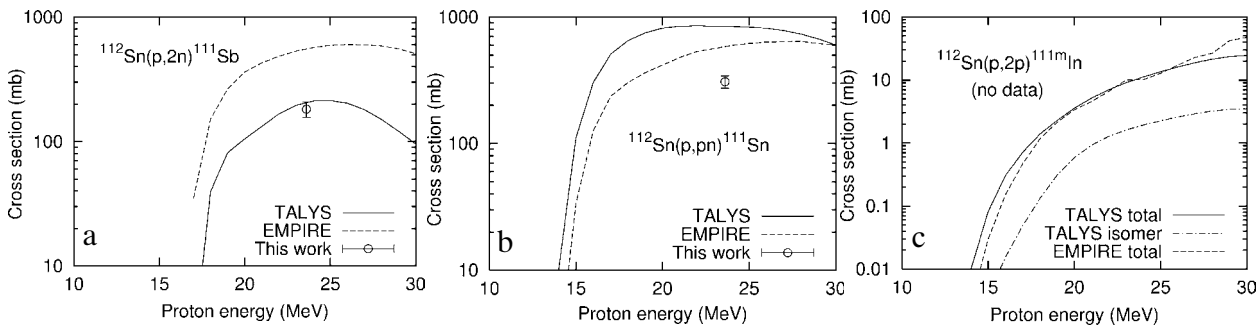

Fig. 7. Calculated excitation functions for the ^{112}Sn(p,2n)^{111}Sb (a) and ^{112}Sn(p,pn)^{111}Sb (b) reactions and experimental cross sections for these reactions at E_p = 23.6 MeV proton energy. Both reactions lead to the ^{111}In formation indirectly. (c) Shows the excitation function of the ^{112}Sn(p,2p)^{111}In reaction leading directly to the ^{111}In formation, but unfortunately the experimental cross sections for this reaction are unknown. Here, the EMPIRE code has been able to give only the total cross section, i.e. the sum of cross sections to the ground and to the isomer states, whereas the TALYS calculations could separate both parts. The calculations of the total cross sections using both codes are in very good mutual agreement.

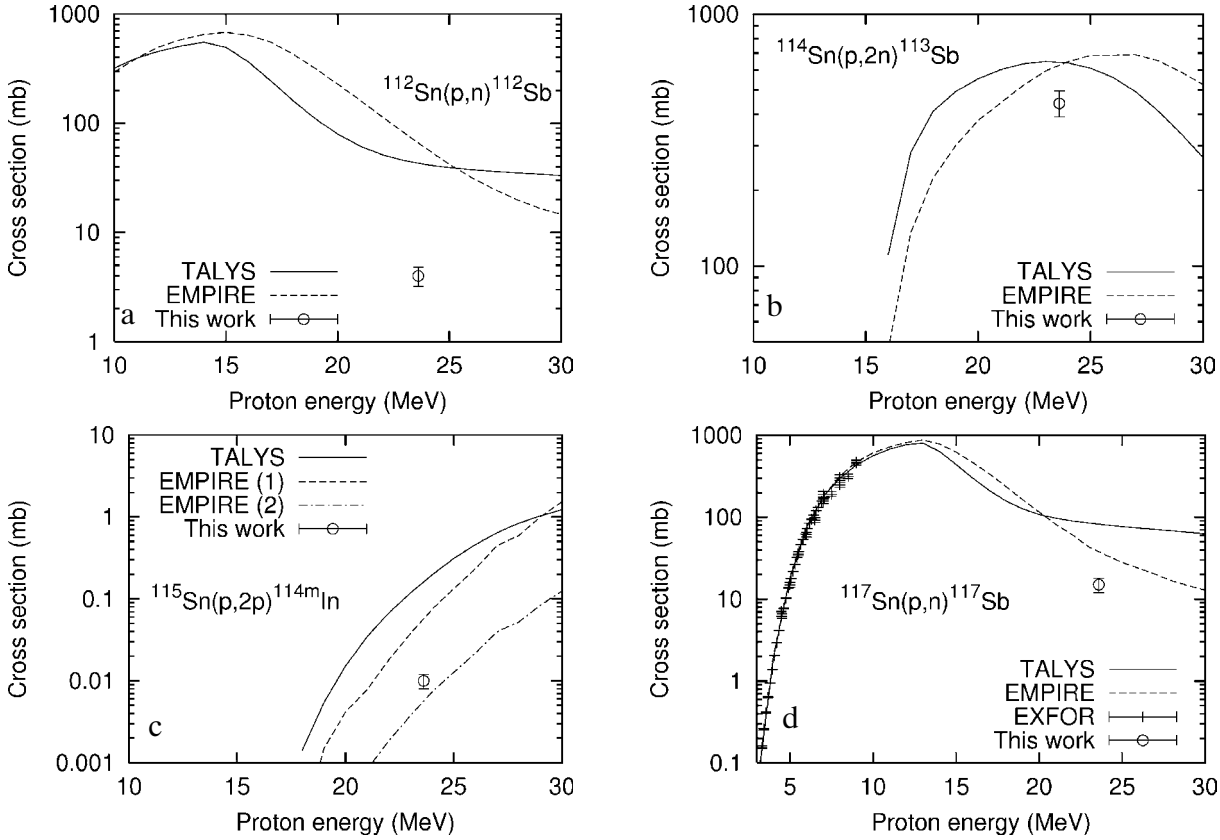

Fig. 8. Calculated excitation functions for reactions competing with the ^{111}In production during proton bombardment of 84% enriched ^{112}Sn sample. (a) The excitation function for the ^{112}Sn(p,n)^{112}Sb reaction with our experimental cross section for this reaction at 23.6 MeV proton energy. (b) The same for the ^{114}Sn(p,2n)^{113}Sb reaction. (c) The contribution of the ^{115}Sn(p,2p)^{114}In reaction to the ^{114m2}In production is small since the total cross section σ_t is rather low. The EMPIRE calculations do not yield here the isomer state production including the de-excitation of states populated in ^{114}In. The upper curve (EMPIRE(1)) is the sum of production of the isomer and the ground states of ^{114}In, whereas the lower one (EMPIRE(2)) is the direct population of the isomer state in the reaction, without the successive depopulation by γ cascades, which increases the final isomeric yield. The experimental cross section for the excitation of the 50 day isomeric activity σ_m in ^{114}In at E_p = 23.6 MeV is shown here as well. (d) The excitation function of the ^{117}Sn(p,n)^{117}Sb reaction with our experimental cross section for this reaction at E_p = 23.6 MeV proton energy and the EXFOR data [8] at energies below 10 MeV.

All peaks of ^{111}In can be readily distinguished (i.e. 171.3 and 245.4 keV and the summation-coincidence peak at 415.7 keV). Due to the admixture of other Sn isotopes in our 84% enriched ^{112}Sn sample, the ^{117m}Sn (158.6 keV) and ^{113}Sn/^{113m}In (255 and 391.7 keV) activities are also formed and have been properly identified. The remaining γ-lines belong to the background.

A comparison of some yields reported elsewhere [32] with the data obtained in this work is given in Table 2.

Considering the threshold energies and the values of cross sections of the reactions leading to ^{111}In formation the major contributing processes are ^{112}Sn(p,pn)^{111}Sn → ^{111}In (significant production of ^{111}Sn begins at 15 MeV proton energy) and ^{112}Sn(p,2n)^{111}Sb → ^{111}Sn → ^{111}In. A comparison of the calculated excitation functions of these two reactions and of our data determined at proton energy 23.6 MeV shows (Fig. 7) that the ^{112}Sn(p,2n)^{111}Sn process has two times higher cross section than the ^{112}Sn(p,2n)^{111}Sb reaction in the energy region considered. Special consideration should be given to the ^{112}Sn(p,2p)^{111}In reaction, since this one leads to the direct formation of ^{111}In. However, the calculations (Fig. 7c) indicate that the cross sections in the energy region of interest are small, not exceeding few mb. The experimental cross section for this reaction is difficult to measure and it is unknown up to now. The low contribution of this reaction to the ^{111}In production can be neglected. These excitation functions are given in Fig. 8.

Yield and purity of ^{111}In

About 1.6×10^5 Bq (4.4 μCi) of ^{111}In was obtained during 1 h irradiation with 3.5 nA proton beam current in our experimental conditions (84% enriched 20.6 mg metallic ^{112}Sn sample). Although it is risky to extrapolate linearly the low current yield to production ratio, it was interesting to answer how high the yield would be for proton beams up to 1 μA. Therein, the expected yield is about 46 MBq/μAh (1.2 mCi/μAh). This value of yield for the precursor production of ^{111}In is located between the yield of the ^{111}Cd(p,n)^{111}In and ^{112}Cd(p,2n)^{111}In reactions (see Table 3) using a medium size cyclotron ($E_p \leq 30$ MeV).

As has been pointed out above, the ^{114m2}In contamination must not exceed 0.2% [7]. The radionuclide purity of the ^{111}In radioisotope was ascertained by

Table 2. Measured ^{111}In yield in some nuclear reactions

Target and % of enrichment	Nuclear reaction	Beam energy (MeV)	^{111}In yield (μCi/μAh)	^{114m}In impurity (% of ^{111}In activity)	^{114m}In contribution (% of the ^{111}In dose)
^{nat}Cd	(p,n)	15	140	3	71
^{nat}Cd	(p,2n)	22	1035	0.5	29*
^{111}Cd (96.5)	(p,n)	16	515	0.012	1
^{112}Cd (97)	(p,2n)	27	6000	0.003	0.24
^{113}Cd (95.8)	(p,3n)	63	16,500	0.024	1.88
^{114}Cd (98.9)	(p,4n)	63	15,600	0.26	17.2
^{nat}Cd	(p,xn)	63	10,400	0.6	33
^{112}Sn (84)	(p,pn), (p,2n)	25	1200**	0.0006	0.005***
^{nat}Cd	(d,n)	12	117	5.7	82
^{nat}Ag	(α,2n)	24	64	not detected	–

The ^{111}In yields refer to single energy given in column 2 of the table. Data on reactions on Cd and Ag targets were taken from Ref. [32].
* The data in parentheses were obtained by extrapolating the results of Ref. [6].
** Extrapolated from low current yield.
*** Present work.

Table 3. Threshold energies and cross section of proton-induced reactions on tin isotopes

Nuclear reaction	Threshold energy* (MeV) [2]	Product nuclide	Reaction c.s. (mb)
^{112}Sn(p,n)	8.38	^{112}Sb	4 ± 0.8
^{112}Sn(p,2n)	16.82	^{111}Sb	182 ± 26
^{112}Sn(p,pn)	10.68	^{111}Sn	307 ± 35
^{114}Sn(p,2n)	15.12	^{113}Sb	442 ± 52
^{117}Sn(p,n)	2.56	^{117}Sb	15 ± 3
^{117}Sn(p,p'γ)	–	^{117m}Sn	0.37 ± 0.04
^{115}Sn(p,2p)	8.83	^{114m}In	0.01 ± 0.002

* The threshold energies in this table were calculated considering the energy balance (Q-values). These were taken from Ref. [2].

examining its γ-ray spectrum using both HPGe(Li) spectrometers. Impurities of ^{111}In arise from other tin isotopes, which exist in the enriched ^{112}Sn sample. The extent of ^{114m2}In contamination was determined from the spectrum taken 47 days after EOB (end-of-bombardment), when the 191 keV peak of ^{114m2}In was easily resolved. The effect of sum-up of kX-rays with 171.3 keV γ-line of ^{111}In masked its existence in the γ-ray spectrum obtained few days after EOB. A long-time interval allowed us to determine the ^{114m2}In activity accurately. A typical spectrum of γ-ray activities observed in ^{112}Sn sample 47 days after EOB is shown in Fig. 9.

Discussion

A strongly pronounced 158 keV photopeak was observed at a long-time measurement of the ^{111}In activity. Its decay was not a single exponential one. Thus, an analysis was necessary to determine the details. Our 84% enriched sample contains 0.25% of ^{117}Sn, and the ^{117}Sn(p,n) reaction produces ^{117}Sb ($T_{1/2}$ = 2.8 h), which essentially (I_γ = 85.9%) produces gammas of 158.5 keV. The 158.6 keV γ is emitted by ^{117}Sn(p,p'γ)^{117m}Sn (I_γ = 86.4%). The Ge(Li) detector is unable to resolve these two peaks, but the time-dependences of their decay curves can be – due to significantly different lifetimes – successfully used to separate these two activities. The ^{114m2}In activity is the last one, but the most important stuff from the point of view of the ^{111}In contamination. The cross section for the isomeric state of ^{114}In has been measured using 190.3 keV γ-ray emitted during decay to the ground state ($T_{1/2}$ = 71.9 s). So far, the excitation functions have not been investigated experimentally for all reactions presented in Table 4.

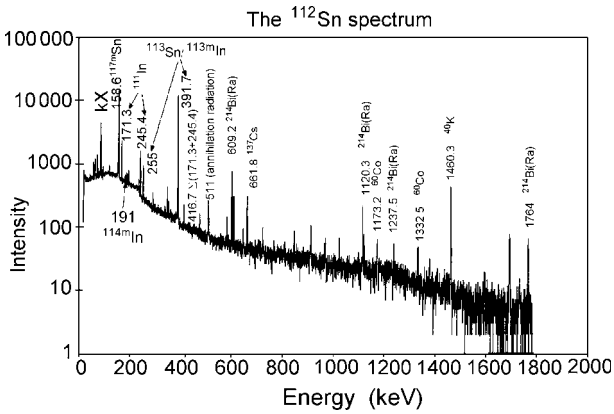

Fig. 9. The gamma-ray spectrum of nuclides produced in the 84% enriched metallic ^{112}Sn sample irradiated with 24.4 MeV protons during 1 h. Delay time 48 days, measuring time 18 h using a 72 cm^3 HPGe detector of the Radioisotope Centre (Polatom, Świerk). The 190.3 keV peak of ^{114m2}In can just be recognized with certainty in this spectrum. Besides the ^{114}In activity, we can see ^{117m}Sn and ^{113}Sn/^{113m}In activities (the 158.6, 255 and 391.7 keV gamma-lines, respectively). The remaining prominent gamma-lines belong to the background.

Table 4. Properties of radionuclides produced after short (5 min) and long (1 h) irradiation of the 84% enriched ^{112}Sn sample, their half-lives and the γ-rays used to determine the activity

Nuclear reaction	Product nuclide	Properties of product nuclide		
		$T_{1/2}$ [30]	E_γ (keV) [22]	I_γ (%) [22]
^{112}Sn(p,n)	^{112}Sb	51.4 s	990.9 1257.1	14.3 96.0
^{112}Sn(p,2n)	^{111}Sb	75 s	154.5	67.0
^{112}Sn(p,pn)	^{111}Sn	35.3 min	762.0 1153.0	1.48 2.7
^{114}Sn(p,2n)	^{113}Sb	6.67 min	498.0	80.0
^{117}Sn(p,n)	^{117}Sb	2.80 h	158.6	85.9
^{117}Sn(p,p'γ)	^{117m}Sn	13.76 d	156.0 158.6	2.11 86.4
^{115}Sn(p,2p)	^{114m}In	49.51 d	190.3	15.1

The ^{117}Sn(p,n) reaction at incident energies below 10 MeV, where the experimental data are available [8], is an exception here.

Uncertainties in the cross sections reported in the present work are composed of uncertainties from various sources entering the well known activation formula. The most important ones are: i) photopeak counting statistics both from the radionuclide investigated and the background ones; ii) uncertainty in the absolute efficiency determination of the HPGe detector; iii) the error of total number of protons on the target (mainly due to the error of the monitor reaction cross sections); iv) the errors in the decay data (half-lives and/or branching ratios). Other uncertainties such as those of proton beam energies, sample weight, isotopic abundance, and irradiation, cooling and measuring times were small (of the order of 0.1% to 1%). The effect of beam inhomogeneity is very difficult to estimate. Since the individual errors are independent, and they vary from radioisotope to radioisotope, the total error in the cross sections is obtained by taking the square root of the sum of the squares of the individual errors. They are of three types: some of them (e.g. the detector efficiency or the sample weight) are well estimated; some others (e.g. statistical uncertainty) are evaluated; and the remaining ones (e.g. monitor reaction cross section or nuclear decay data) are considered as fixed in calculating the resulting total error. This can reach about 20% in unfavourable cases (short lifetime, low cross section and small abundance in the sample), whereas in the favourable ones the total error is about 11%.

One of the most important parameters in the determination of a cross section is the measurement of the beam current incident on each foil. The proton beam was monitored as described above and using Ni foils for the irradiation of ^{112}Sn sample. However, for Ni monitoring foil, no inconsistency in the integrated beam current was observed when monitor reactions leading to ^{57}Co, ^{57}Ni and ^{61}Cu activities were used, except for the ^{55}Co activity. We therefore conclude that the published experimental cross sections for monitoring reaction ^{nat}Ni(p,X)^{55}Co at 22.6 ± 0.3 MeV proton energy, namely 9 ± 0.87 mb [29], is too low. We remeasured this activity and arrived to 36.6 ± 4 mb at E_p = 22.8 MeV. This value is in good agreement with Refs. [16, 20]. The ^{60}Cu activity ($T_{1/2}$ = 23.2 min) is also formed at proton irradiation of the ^{nat}Ni foil. The ^{60}Cu nucleus populates a large number of γ transitions (E_γ = 467–3269 keV) including some high-energy ones, which make it easy to detect and identify. We have found only two papers [5, 28] of earlier cross section measurements of proton induced reactions on Ni leading to the ^{60}Cu formation. Tanaka *et al.* [28] measured the cross sections of the ^{60}Ni(p,n)^{60}Cu reaction in the energy range 7 to 15 MeV using 99.1% enriched ^{58}Ni target; Blosser and Handley [5] gave the cross section of the ^{60}Ni(p,n)^{60}Cu at a proton energy of 12 MeV. The ^{60}Ni(p,n)^{60}Cu (Q = –6.9 MeV) and ^{61}Ni(p,2n)^{60}Cu (Q = –14.7 MeV) reactions are expected to contribute to the formation of ^{60}Cu using natural Ni target in our experiment. Taking into account the isotopic composition of ^{nat}Ni target (26.2% of ^{60}Ni and 1.14% of ^{61}Ni) and the reaction Q-values, the contribution of the ^{61}Ni(p,2n)^{60}Cu reaction is rather small. The cross section of the ^{nat}Ni(p,X)^{60}Cu reaction was measured using the 826.4 and 1791.6 MeV γ-rays emitted in the decay of ^{60}Cu at proton energy E_p = 22.8 MeV and it is equal to 64.4 ± 7 mb.

In the ^{111}Sn → ^{111}In decay chain, the maximum activity of daughter isotope occurs at time t_m equal to 4 h after the end-of-bombardment (EOB) [4]. The amounts of ^{111}In and the ^{114m2}In impurity were calculated for t_m = 5 h (see Fig. 9), although the die-out of the ^{111}Sn activity is t = 13.5 h. The ^{111}In produced by the 24.4 MeV proton bombardment of the 84% enriched ^{112}Sn contains 0.000625% of ^{114m2}In. This isotope with its half-life 49.51 days gives approximately 80 times the dose per 37 MBq millicurie of ^{111}In required for patient examination [7]. Taking into account the 0.000625% contamination of ^{111}In by ^{114m2}In, the activity ratio is $A(^{114m2}\text{In})/A(^{111}\text{In})$ = 0.00000625 and the dose ratio is $D(^{114m2}\text{In})/D(^{111}\text{In})$ = 0.00000625 × 80 = 0.0005. Therefore, the total dose ratio is $D(^{114m}\text{In})/[D(^{111}\text{In} + D(^{114m2}\text{In})]$ = [0.0005/(0.0005 + 1)] = 0.00049975 ≅ 0.0005. So, in our case with 0.000625% contamination,

the ^{114m2}In contributes by 0.05% to the total dose (medical requirements of 0.2% imply this value to be 14%). Therefore, the ^{111}In formation with 25 MeV protons via radioisotope precursor system ^{111}Sb → ^{111}Sn → ^{111}In is the most suitable method of production of high purity ^{111}In. The relatively high percentage (0.017%) of $A(^{113}\text{Sn})/A(^{111}\text{In})$ is not disturbing at all due to the separation of indium from the tin target. The other important impurity ^{113m}In from the decay of ^{113}Sn may be observed together with ^{111}In after separation but it disappeared almost completely one day after EOB due to the short half-life of ^{113m}In ($T_{1/2}$ = 99 min). In Fig. 5a clearly demonstrates that separation of ^{111}In from the target should be done at the maximum of ^{111}In activity, i.e. about four or five hours after the EOB, because long-lived ^{113}Sn activity slowly increases with time.

Conclusions

We have performed experiments to find out a simple and efficient way of the ^{111}In production via the ^{111}Sb → ^{111}Sn → ^{111}In reaction with the highest purity product and practically free of the ^{114m2}In contaminant. It uses the decay of the ^{111}Sn parent and the ^{111}Sb grandparent radioisotopes formed in the ^{112}Sn(p,pn)^{111}Sn and ^{112}Sn(p,2n)^{111}Sb reactions. The decay period of the ^{111}Sn may be utilized for transport of the ^{111}Sn/^{111}In radionuclide pair from the product site to a distant radiopharmaceutical laboratory. We measured cross sections of both reactions using 84% enriched ^{112}Sn metallic sample at 23.6 MeV proton energy. Many radioisotopes other than ^{111}Sb, ^{111}Sn and ^{111}In are also produced in the sample through various nuclear reactions but without influence on the purity of ^{111}In produced. We have also measured the cross sections for reactions leading to excitation of these accompanying radioisotopes. Analysis of cross sections and half-lives indicated that the ^{112}Sn(p,pn)^{111}Sn reaction is one of the principal reaction channels producing high purity ^{111}In.

There is a need for detailed excitation function measurements for the ^{112}Sn(p,*x*p*y*n) reactions in the energy range from threshold up to 30 MeV. As we did not have enough ^{112}Sn foils, it was not possible to measure very interesting excitation functions of the (p,pn) and (p,2n) reactions on the ^{112}Sn targets. The excitation functions of the above-mentioned reaction channels and of accompanying reactions were calculated with the use of the sophisticated nuclear reaction codes EMPIRE-II (v. 2.19) and TALYS and compared to our experimental data.

The criteria for the selection of one of two processes leading to ^{111}In production, i.e. directly via the ^{111,112}Cd(p,*x*n)^{111}In (x = 1,2) reactions or indirectly via the ^{112}Sn(p,2n)^{111}Sb → ^{111}Sn → ^{111}In and ^{112}Sn(p,pn)^{111}Sn → ^{111}In reactions, for use at a medium-sized cyclotron would be, as ever, the yield and the radionuclide purity of ^{111}In, but determined experimentally for fluence of the proton beams of 1 μAh or more.

Acknowledgment We express our thanks to J. Olszewski for making drawings of experimental arrangement, M. Matul for determination the absolute efficiency of Ge(Li) detector and H. Trzaskowska for preparation of remaining drawings for our publication. The authors also wish to thank E. Kołakowska for her help in the measurements of the activities in the tin samples for a period of seven weeks using the Radioisotope Centre Ge(Li) spectrometer. We are also grateful to the referee of this paper for comments which helped us to improve the presentation of our results. The work has been supported in part by the Slovak grant agency VEGA, grant No. 2/4102 and by the IAEA contract No. 12425/R2.

References

1. Aleksandrov VN, Siemienova MP, Siemienov VG (1987) Cross sections for radionuclide production in the (p,*x*) reactions on Cu and Ni nuclei. Atomnaya Energiya 62:411–413 (in Russian)
2. Audi G, Wapstra AH, Thibault C (2003) The AME2003 atomic mass evaluation II. Tables, graphs and references. Nucl Phys A 729:337–676
3. Běták E (2006) Model calculations of radiative capture of nucleons in MeV region. AIP Conf Proc 819:226–230
4. Běták E, Mikołajczak R, Staniszewska J, Mikołajewski S, Rurarz E (2005) Activation cross sections for reactions induced by 14 MeV neutrons on natural tin and enriched ^{112}Sn targets with reference to ^{111}In production via isotope generator ^{112}Sn(n,2n)^{111}Sn → ^{111}In. Radiochim Acta 93:311–326
5. Blosser HG, Handley TH (1955) Survey of (p,n) reactions at 12 MeV. Phys Rev 100:1340–1344
6. Dahl JR, Tilbury RS (1972) The use of a compact, multiparticle cyclotron for the production of ^{52}Fe, ^{67}Ga,^{111}In and ^{123}I for medical purposes. Int J Appl Radiat Isot 23:431–437
7. European Pharmacopoeia, 3rd ed. (2000) Supplement 2000. Council of Europe, Strasbourg
8. EXFOR (2005) EXFOR-CINDA for applications. Database and retrieval systems, v. 1.63i (CD ROM). IAEA, Vienna (http://www-nds.iaea.or.at/exfor)
9. Firestone RB, Shirley V (1996) Table of isotopes, 8th ed. John Wiley & Sons, New York. Vol. 1
10. GENIE (2000) User's manual, basic spectroscopy software and documentation for Genie 2000 software suite. Canberra Industries 800 Research Parkway, Meridan, Connecticut 06450, USA
11. Grutter A (1982) Excitation functions for radioactive isotopes produced by proton bombardment of Cu and Al in the energy range of 16–70 MeV. Nucl Phys A 383:98–108
12. Gul K (2001) Calculations for the excitation functions of the ^{63}Cu(p,n)^{63}Zn, ^{63}Cu(p,n)^{62}Zn and ^{65}Cu(p,n)^{65}Zn reactions. Appl Radiat Isot 54:147–151
13. Herman M (2002) EMPIRE-II statistical model code for nuclear reaction calculations (version 2.18 Mondovi). IAEA, Vienna
14. Herman M, Obložinský P, Capote R *et al.* (2005) EMPIRE modular system for nuclear reaction calculations (version 2.19 Lodi). NNDC BNL, Upton, USA
15. Janni JF (1982) Proton range-energy tables, 1 keV – 1 GeV. Part 1. At Data Nucl Data Tables 27:147–339
16. Kaufman S (1960) Reactions of protons with ^{58}Ni and ^{60}Ni. Phys Rev 117:1532–1538

17. Koning AJ, Delaroche JP (2003) Local and global nucleon optical models from 1 keV to 200 MeV. Nucl Phys A 713:231–310
18. Koning AJ, Hilaire S, Duijvestijn MC (2004) TALYS: a nuclear reaction program. Report 21297/04.62741/P FAI/AK/AK. NRG, Petten
19. Kopecky P (1985) Proton beam monitoring via the Cu(p,x)^{58}Co, ^{63}Cu(p,2n)^{62}Zn, and ^{65}Cu(p,n)^{65}Zn reaction in copper. Int J Appl Radiat Isot 36:657–661
20. Michel R, Weigel H, Herr W (1978) Proton induced reaction on nickel with energies between 12 and 45 MeV. Z Phys A 286:393–400
21. Novgorodov AF, Biełov AG, Zieliński A, Kołaczkowski A (1987) A simple method for high-temperature separation of ^{111}In from massive tin targets. Radiochimiya 29:254–258 (in Russian) (also see: preprint P6-85-918, JINR Dubna)
22. NuDat 2.1, http://www-nds.iaea.org/nudat2/index.jsp
23. Radionuclide transformations. Energy and intensity emissions (1983) Annals of the ICRP no. 38. Pergamon Press, Oxford-New York-Frankfurt
24. Reus U, Westmeier W (1983) Catalog of γ-rays from radioactive decay. At Data Nucl Data Tables 29:193–406
25. RIPL-2 (2006) Handbook for calculations of nuclear reaction data. Reference input parameter library. IAEA-TECDOC-1506. IAEA, Vienna (http://www-nds.iaea.or.at/ripl-2/)
26. Rurarz E, Mikołajewski S (1993) Model calculations of ^{111}In production via the ^{112,114,115,116,117}Sn(p,xnypza)^{111}Sb → ^{111}Sn → ^{111}In reactions. Report SINS 02147/II. Soltan Institute for Nuclear Studies, Świerk, Poland
27. Schwerer O, Okamoto K (1989) Status report on cross sections on monitor reactions for radioisotope production. Report INDC(NDS)-21 GZ+. IAEA, Vienna
28. Tanaka S, Furukawa M, Chiba M (1972) Nuclear reactions of nickel with protons up to 56 MeV. J Inorg Nucl Chem 34:2419–2426
29. Tarkányi F, Szelecsenyi F, Kopecky P (1991) Excitation functions of proton induced nuclear reactions on natural nickel for minitoring of beam energy and intensity. Appl Radiat Isot 42:513–517
30. Tuli JK (2005) Nuclear wallet cards. BNL, Upton, NY
31. Williamson CF, Bujot JP, Picard J (1966) Tables of range and stopping power of chemical elements for charged particles of energy 0.5 to 500 MeV. Report CEA-R-3042. CEA, Saclay
32. Zaitseva NG, Knotek O, Kowalew A *et al*. (1990) Excitation functions and yields for ^{111}In production using ^{113,114,nat}Cd (p,xn)^{111}In reaction with 65 MeV protons. Appl Radiat Isot 41:177–183